

Synthesis and Lithium Storage Performance of CoO/CoSe Composite Nanoparticles Supported on Carbon Paper

Suyang Song, Xinhua Xu, Shengyi Shi and Xingqun Zhu *

School of Materials Science and Engineering, Xuzhou University of Technology, Xuzhou, Jiangsu 221018, China

* Corresponding author: Xingqun Zhu

Abstract

For high-performance lithium-ion battery applications, this study successfully constructed a self-supported composite electrode with CoO/CoSe heterostructure nanoparticles loaded on carbon paper via a two-step hydrothermal-selenization method. XRD and SEM characterizations confirmed the uniform distribution of CoO/CoSe nanoparticles on the carbon paper fibers, forming a robust 3D porous conductive network. Electrochemical tests demonstrated the superior performance of this composite electrode: in galvanostatic charge/discharge, cyclic voltammetry, and rate capability tests, its lithium storage capacity, cycling stability, and rate performance significantly outperformed those of non-self-supported CoO/CoSe materials. The performance enhancement mechanism arises from the structural advantages: the CoO/CoSe heterointerface accelerates ion/electron kinetics, while the carbon paper backbone provides rapid electron transport pathways and effectively mitigates electrode volume expansion to maintain structural integrity. The developed carbon paper-based CoO/CoSe self-supported anode addresses the key bottlenecks of slow ion diffusion and large volume expansion in conventional anode materials through the synergistic effect of heterostructure design and 3D conductive architecture, exhibiting high specific capacity, long cycle life, and excellent rate capability. This strategy provides an effective approach for developing next-generation high-performance lithium-ion battery anodes with significant application potential. Future work will focus on optimizing the fabrication process and advancing practical full-cell studies.

Keywords

Lithium-ion Batteries; Composite Nanoparticles; CoO/CoSe; Heterogeneous Structure.

1. Introduction

In recent years, transition metal oxides (e.g., CoO, theoretical capacity of 715 mAh/g) and transition metal selenides (e.g., CoSe, theoretical capacity of 389 mAh/g) have attracted significant attention as promising anode materials owing to their high specific capacity and excellent redox activity [1-3]. The lithium storage mechanism of CoO involves a conversion reaction ($\text{CoO} + 2\text{Li}^+ + 2\text{e}^- \rightarrow \text{Co} + \text{Li}_2\text{O}$), which facilitates multi-electron transfer, thereby significantly enhancing energy density [4]. However, practical applications of CoO anodes face two major challenges: (1) Reversible formation and decomposition of Li_2O are accompanied by large volume changes, which can lead to a loss of electrical contact between particles and hence to capacity fading [5]; and (2) the intrinsically low electrical conductivity of metal oxides/selenides hinders efficient electron transport, adversely affecting the rate capability and cycling stability of CoO-based anodes.

In contrast, transition metal selenides like CoSe, with their metal-like conductivity (electrical conductivity $>10^3$ S/cm) and structural stability, are considered ideal anode materials. The

lithium storage mechanism of CoSe involves a combination of alloying reaction ($\text{CoSe} + x\text{Li}^+ + xe^- \rightarrow \text{Co} + \text{Li}_x\text{Se}$) and partial conversion reaction [6]. Moreover, the layered crystal structure of CoO (similar to MoS_2) helps alleviate volume strain during lithiation. Volume strain can cause internal fracture of anode particles or detachment of the solid electrolyte interphase (SEI) layer from the particle surface. In either case, the exposed electrode surface forms new SEI layers repeatedly, accelerating electrode aging and leading to significant degradation in battery performance, such as capacity loss. However, CoSe's unique structure effectively mitigates electrode aging.

Despite these advantages, both materials still face challenges in practical applications: (1) volume changes induced by lithium-ion movement during charge/discharge processes, causing electrode pulverization and failure; and (2) the low conductivity of metal oxides and the limited capacity of selenides, both of which impair battery performance to varying degrees. To address these issues, Nanostructure engineering (e.g., MOF-derived porous frameworks) and 3D conductive substrates (e.g., graphene aerogels, carbon cloth) are proven strategies to enhance mechanical stability. For example, a research team from Peking University employed a metal-organic framework (MOF) template to synthesize multilayered porous CoSe nanopolyhedrons. The material's high specific surface area and abundant active sites enhanced polysulfide conversion efficiency, achieving an initial capacity of 1634.9 mAh/g in lithium-sulfur battery cathodes with only 0.04% capacity decay after 1200 cycles [7]. Similarly, Prof. Xiong Wen (David) Lou's group at Nanyang Technological University designed a multi-channel carbon fiber-supported $\text{CoS}_2/\text{SeS}_2$ composite, utilizing a 3D conductive network and chemical adsorption to suppress the shuttle effect. This enabled a high sulfur loading (2.5 mg/cm^2) while maintaining a capacity of 745 mAh/g after 100 cycles [8]. These studies demonstrate that modifying electrode materials with nanostructures offers multiple advantages: Nanostructured particles typically exhibit excellent conductivity, small size, and high surface area, which significantly increase the number of active sites, thereby improving specific capacity. Additionally, they facilitate the rapid formation and stabilization of the SEI layer, reducing electrolyte consumption and enhancing cycling stability. Leveraging the size effect of nanoparticles, the diffusion path of lithium ions during insertion/extraction can be shortened, while volume expansion is alleviated, thereby improving ion diffusion rates and charge/discharge efficiency [9].

To further enhance anode material performance, researchers have explored carbon-based composite anodes. Constructing CoO/CoSe heterostructures can combine the high theoretical capacity of CoO with the superior conductivity of CoSe, leveraging synergistic effects to improve electrode conductivity, suppress volume expansion, and maintain high capacity, ultimately boosting lithium storage performance [10]. Carbon-based substrates (e.g., carbon paper) not only enhance conductivity but also provide mechanical support for active materials through their 3D porous structure, mitigating volume expansion while enabling fast electron/ion transport [11]. In recent years, heterojunction composites (e.g. CoO/CoSe) have exhibited superior electrochemical performance compared to single-component materials due to interfacial synergistic effects, such as built-in electric fields facilitating charge transfer [12,13]. This work proposes the construction of transition metal cobalt oxide and selenide nanoparticles and investigates their lithium storage performance. The main focus is on the preparation of carbon paper-supported CoO/CoSe composite nanoparticles and the study of their lithium storage properties. The proposed method involves loading Co-containing precursor nanoparticles onto carbon paper via a hydrothermal process, followed by high-temperature selenization to obtain carbon paper-supported CoO/CoSe composite nanoparticles. These will be used as self-supported electrodes to assemble coin-type half-cells for studying lithium-ion storage performance. Carbon paper, as a carrier material with high conductivity, excellent mechanical properties, and chemical stability, demonstrates significant

potential in electrode material applications. Its inherent three-dimensional (3D) porous architecture provides not only a large surface area for active material loading but also establishes efficient pathways for electron transport and ion diffusion [14]. By loading CoO/CoSe composite nanoparticles onto carbon paper to form a self-supported electrode, the need for traditional electrode components such as current collectors and binders can be eliminated, thereby improving battery energy density. Furthermore, the construction of a CoO/CoSe heterostructure combines the advantages of both materials, leveraging synergistic effects to enhance electrode conductivity, suppress volume expansion, and maintain high capacity, ultimately improving lithium storage performance. This approach provides new insights and directions for the development of high-performance lithium-ion battery electrode materials.

2. Experimental Section

2.1. Chemicals and Materials

Cobalt acetate ($\text{Cu}(\text{CH}_3\text{COO})_2 \cdot \text{H}_2\text{O}$, AR) was purchased from Sinopharm Group Chemical Reagent Co., LTD. Urea was purchased from Xilong Chemical Co., LTD. Polyethylene glycol (PEG-1000) and selenium (Se) powder were purchased from Shanghai Aladdin Biochemical Technology Co., LTD. The carbon paper (CP, TGP-H-060) was purchased from TORAY Company.

2.2. Preparation of u-CoO/CoSe/CP and up-CoO/CoSe/CP Self-supported Electrodes

Dissolve 0.03mol of cobalt acetate in 30ml of ethanol, then dissolve 1.2 grams of urea in 30ml of distilled water. Mix the two solutions and stir until the solutions are uniform. Then, evenly divide the mixed solution into two parts and pour them into the two reaction vessels A and B. Add 5 to 6 pieces of carbon paper similar in size to the vessel mouth to each reaction vessel. Add 0.01g of polyethylene glycol (PEG-1000) to reaction vessel A. Place both reaction vessels in an electric heating constant temperature air circulation drying oven and heat up to 180°C, then maintain the temperature for 24 hours. Carbon paper (CP) loaded with co-precursor nanoparticles was obtained. The carbon paper from the two reaction vessels was taken out, carefully washed with ethanol and distilled water successively, and then placed in two glass dishes respectively. Finally, the glass dishes were put into a vacuum drying oven and dried at 80°C for one hour. After the drying process is completed, selenization is carried out. Carbon paper from two glass dishes is placed in two quartz boats, and then 3g of Se powder (the mass ratio of Se powder to sample powder =2:1) is weighed and put into one quartz boat as well. Finally, first place the quartz boat containing Se powder about 5 centimeters upstream of the tube furnace from the sample, and then place the quartz boat containing the sample downstream of the tube furnace. The temperature was heated to 800°C in a tubular furnace with an argon atmosphere and held for one hour before cooling. The final product obtained was a carbon paper-loaded CoO/CoSe composite nano self-supported electrode. The final product obtained from the reaction in reactor A was recorded as up-CoO/CoSe/CP. The final product obtained from the reaction in Reactor B is denoted as u-CoO/CoSe/CP.

2.3. The Preparation of the Control Group's Non-self-supported Electrode

During the preparation process of the above-mentioned u-CoO/CoSe/CP and up-CoO/CoSe/CP materials, the solutions in the two reaction vessels A and B after the hydrothermal reaction were subjected to vacuum filtration. The powder samples obtained after filtration were placed in glass dishes and then dried at 80 °C in a vacuum drying oven for one hour. After the drying was completed, selenization was carried out simultaneously with the carbon paper-supported samples. The powder samples obtained from reactors A and B are respectively denoted as up-CoO/CoSe and u-CoO/CoSe. The up-CoO/CoSe and u-CoO/CoSe sample films were coated on

the copper current collector to prepare electrodes: Weigh 0.14 g of the sample powder, along with appropriate amounts of acetylene black and PVDF (mass ratio of sample: acetylene black: PVDF=7:2:1). Grind the mixture while gradually adding N-methylpyrrolidone (NMP) until a homogeneous, particle-free slurry is obtained. Finally, the obtained slurry is evenly coated on the copper foil, and then it is placed in a vacuum oven to dry at 60°C for 12 hours to obtain the electrode material.

2.4. Characterization and Electrochemical Measurements

Scanning electron microscopy (SEM) characterization was conducted using zeiss supra 55 (Oxford Instruments). X-ray diffraction (XRD) measurements were carried out on an Rigaku U IV diffractometer at 40 kV and 20 mA using Cu K α radiation ranging from 10° to 80°. The u-CoO/CoSe/CP, up-CoO/CoSe/CP self-supported electrodes, and non-self-supported electrode were cut into the 12 nm disk to work as an anode electrode and transferred into the glove box. The 2032-type lithium-ion batteries were assembled with our electrodes and lithium tablet, which are used as working and counter electrodes, respectively. The electrolyte was LiPF₆ (1 M) dissolved in the hybrid solvent (1:1:1 vol%) with EC (ethylene carbonate) and DEC (diethyl carbonate). The lithium-ion storage properties were explored with the NEWARE system and CHI 760E workstation.

3. Results and Discussion

Figure 1a shows the XRD pattern of the prepared u-CoO/CoSe/CP composite nanoelectrode sample, the sample presents a very strong diffraction peak at $2\theta \approx 27^\circ$, which is a characteristic peak of carbon paper. Diffraction peaks matching the standard card (PDF#78-0431) of CoO were observed at $2\theta \approx 36.48^\circ$, 42.38° , 61.49° , 73.66° and 77.52° , indicating that CoO was successfully loaded onto the carbon paper with a pure crystal phase free of impurities. The other diffraction peaks belong to CoSe [12,13]. As shown in Figure 1b, the XRD pattern of the up-CoO/CoSe/CP composite nanoelectrode sample is presented. This sample also exhibited a strong diffraction peak belonging to carbon paper at $2\theta \approx 27^\circ$. Diffraction peaks were observed at $2\theta \approx 36.48^\circ$, 42.38° , 61.49° , 73.66° and 77.52° , which were completely consistent with the CoO standard card (PDF#78-0431), confirming the existence of CoO. The diffraction peaks of the sample at $2\theta \approx 33.6^\circ$, 45.2° and 51.2° belong to CoSe (Standard Card (JCPDS#89-2004)) [12,13], indicating the successful synthesis of the CoO/CoSe heterostructure loaded on carbon paper. In addition, the diffraction peak intensities of CoO and CoSe in the up-CoO/CoSe/CP sample are both higher than those in u-CoO/CoSe/CP. This might be because the addition of PEG in the precursor can promote the growth of the material on the carbon paper.

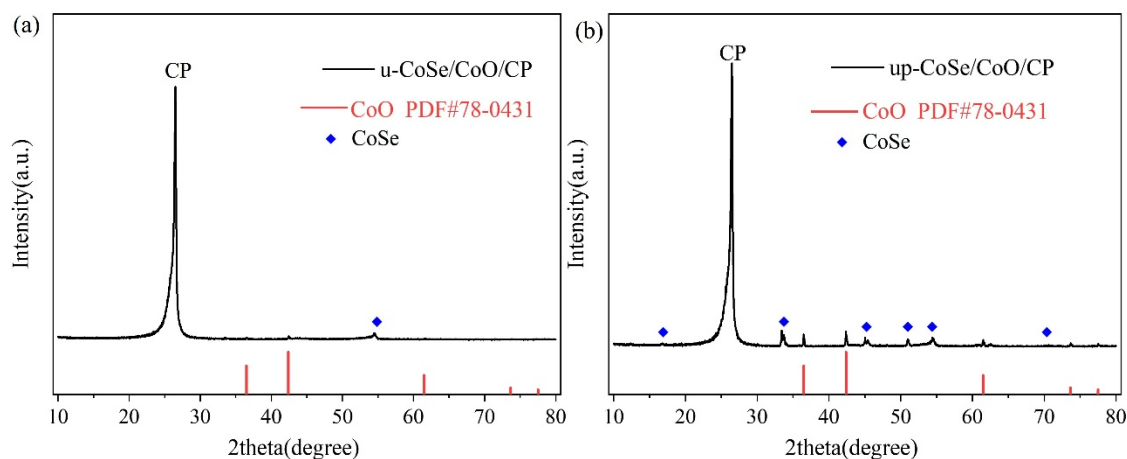


Figure 1. (a) XRD pattern of u-CoSe/CoO/CP and (b) XRD pattern of up-CoSe/CoO/CP.

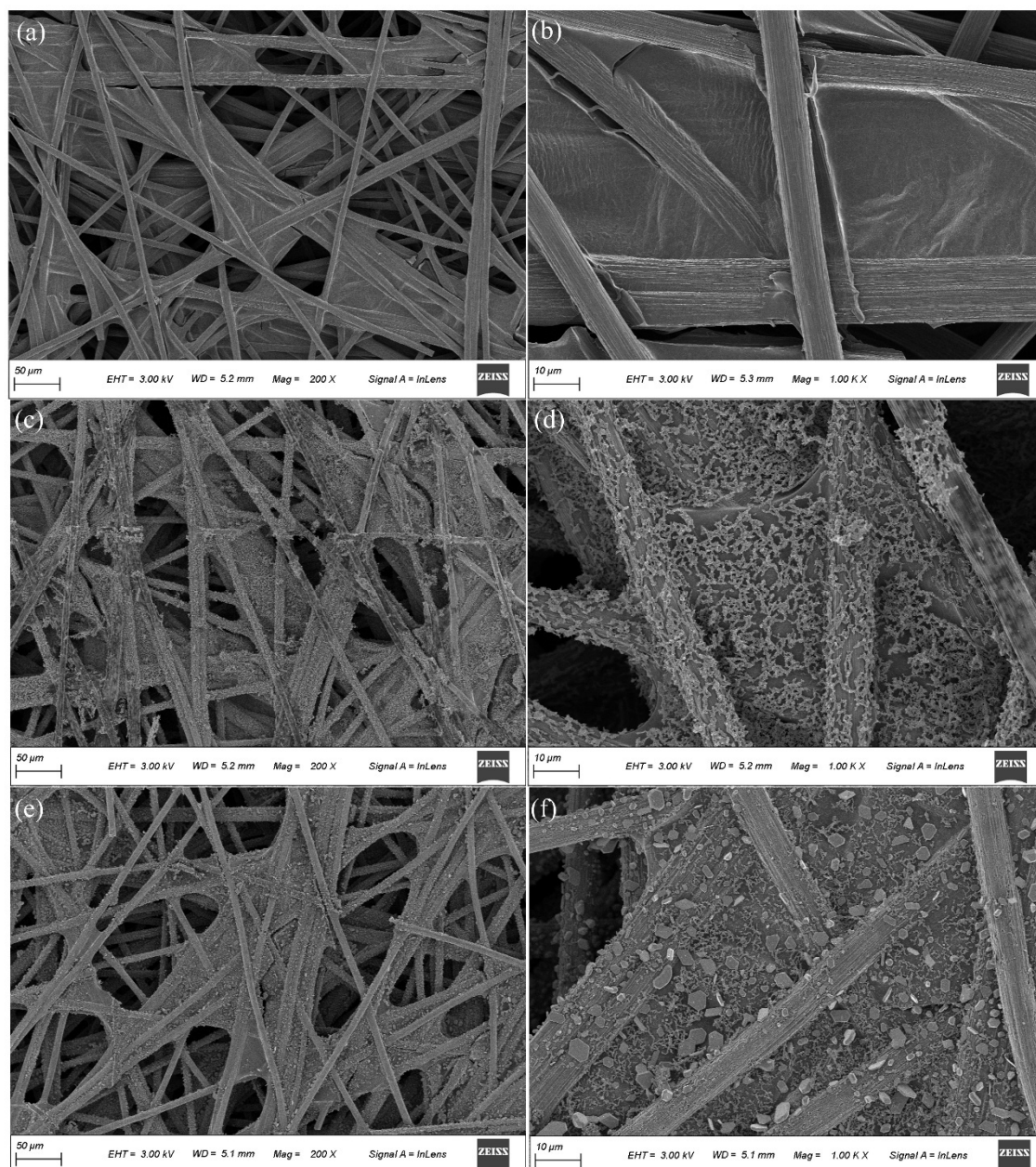


Figure 2. (a) (b), (c) (d), and (e) (f) show the SEM images of blank carbon paper, u-CoSe/CoO/CP, and up-CoSe/CoO/CP at different magnifications, respectively.

The surface morphologies of pristine carbon paper and CoO/CoSe composite nanoparticle loaded on carbon paper samples were investigated using scanning electron microscopy (SEM) as shown in Figure 2. Figure 2a presents a low-magnification (200 \times) view of the blank carbon paper, revealing its characteristic interconnected fibrous network that forms a porous three-dimensional architecture. This unique structure provides both exceptional electrical conductivity and mechanical stability. The higher magnification image (1000 \times , Fig. 2b) shows smooth and featureless fiber surfaces, clearly indicating the absence of any active material deposition. This observation underscores the necessity of applying functional coatings to these carbon fibers to achieve enhanced electrochemical performance. (c-d) u-CoSe/CoO/CP composite electrode: Figure 2c (200 \times magnification) demonstrates successful urea-modified nanoparticle deposition on the carbon paper, the deposited nanoparticles form micron-scale aggregates that display a predominantly uniform distribution, although minor localized agglomeration is evident. As shown in Figure 2d (1000 \times magnification), the high-resolution

view reveals a densely packed nanostructure consisting of 1-2 μm nanoparticles, which collectively generate a highly rough and porous surface morphology. Importantly, the nanoparticles exhibit strong interfacial adhesion to the carbon fibers without any observable delamination, confirming the substrate's ability to provide robust mechanical support for the deposited material. (e-f) up-CoSe/CoO/CP composite electrode (PEG-modified): The incorporation of polyethylene glycol (PEG) induces significant morphology modifications, as evidenced in Figure 2e (200 \times magnification). The modified surface exhibits enhanced smoothness with substantially reduced aggregate dimensions (2-3 μm) and improved spatial uniformity. High-resolution imaging (Fig. 2f, 1000 \times) reveals well-defined spheroidal particles (3-6 μm) displaying both reduced aggregation tendency and decreased surface porosity relative to the unmodified counterpart. These findings demonstrate that PEG serves as an effective surface modifier, establishing a uniform coating layer that simultaneously governs particle growth kinetics and promotes superior dispersion characteristics during synthesis.

The charge/discharge profiles of the u-CoSe/CoO/CP electrode are presented in Figure 3a. The initial cycle exhibits a discharge capacity of approximately 400 mAh/g and a charge capacity of about 380 mAh/g, yielding an impressive Coulombic efficiency (CE) of 95%. Over the subsequent five cycles, the charge and discharge capacities demonstrate remarkable consistency, with the CE progressively approaching 100%. These results indicate outstanding electrochemical stability of the electrode material. This stability can be attributed to the three-dimensional conductive network of the carbon paper substrate, which effectively accommodates volume changes during cycling and prevents the pulverization or delamination of active materials. Figure 3b displays the charge/discharge profiles of the up-CoSe/CoO/CP electrode. The initial cycle demonstrates a discharge capacity of approximately 735 mAh/g and a charge capacity of 745 mAh/g, resulting in a remarkably high first-cycle Coulombic efficiency (CE) of 98.65%. Compared to the u-CoSe/CoO/CP sample (without PEG addition), this modified electrode exhibits significantly enhanced charge-discharge capacity and Coulombic efficiency. Combined with the XRD and SEM analysis, these improvements can be attributed to the higher CoO/CoSe content in the PEG-modified sample. The CoO/CoSe heterostructure synergistically combines the high theoretical capacity of CoO with the superior electrical conductivity of CoSe, leading to enhanced electrode kinetics. Additionally, this heterostructure mitigates volume expansion issues during cycling, thereby improving structural stability and lithium storage performance. Figure 3c presents the cycling performance of the up-CoSe/CoO/CP electrode at a current density of 0.1 A/g, demonstrating exceptional cycling stability. After 100 cycles, the electrode maintains a stable specific capacity of approximately 1000 mAh/g. Figure 3d displays the cycling behavior of the u-CoSe/CoO/CP electrode under the same current density. While this electrode also shows good cycling stability, retaining a capacity of \sim 800 mAh/g after 100 cycles, its performance is slightly inferior to that of the PEG-modified (up-CoSe/CoO/CP) counterpart. This difference can likely be attributed to the more uniform morphology achieved through PEG modification, which enhances structural integrity and electrochemical performance. Figure 3e demonstrates the rate capability of the up-CoSe/CoO/CP electrode. The specific capacity exhibits a stepwise decrease with increasing current density, delivering capacities of 850, 800, 700, 500, 300, and 900 mAh/g at 100, 200, 500, 1000, 2000, and 100 mA/g, respectively. Figure 3f presents the rate performance of the unmodified u-CoSe/CoO/CP electrode. While the specific capacity shows a gradual decline with increasing current density (450, 440, 410, 360, and 465 mAh/g at 100, 200, 500, 1000, and 100 mA/g, respectively), the electrode maintains reasonable capacity retention. This performance demonstrates satisfactory cycling stability and moderate rate capability, though inferior to the PEG-modified system. Comparative analysis reveals that the PEG-modified electrode consistently outperforms its unmodified counterpart in both capacity retention and cycling stability.

Notably, the charge/discharge capacities remain well-matched, suggesting enhanced electrochemical activity and improved reaction reversibility through PEG incorporation.

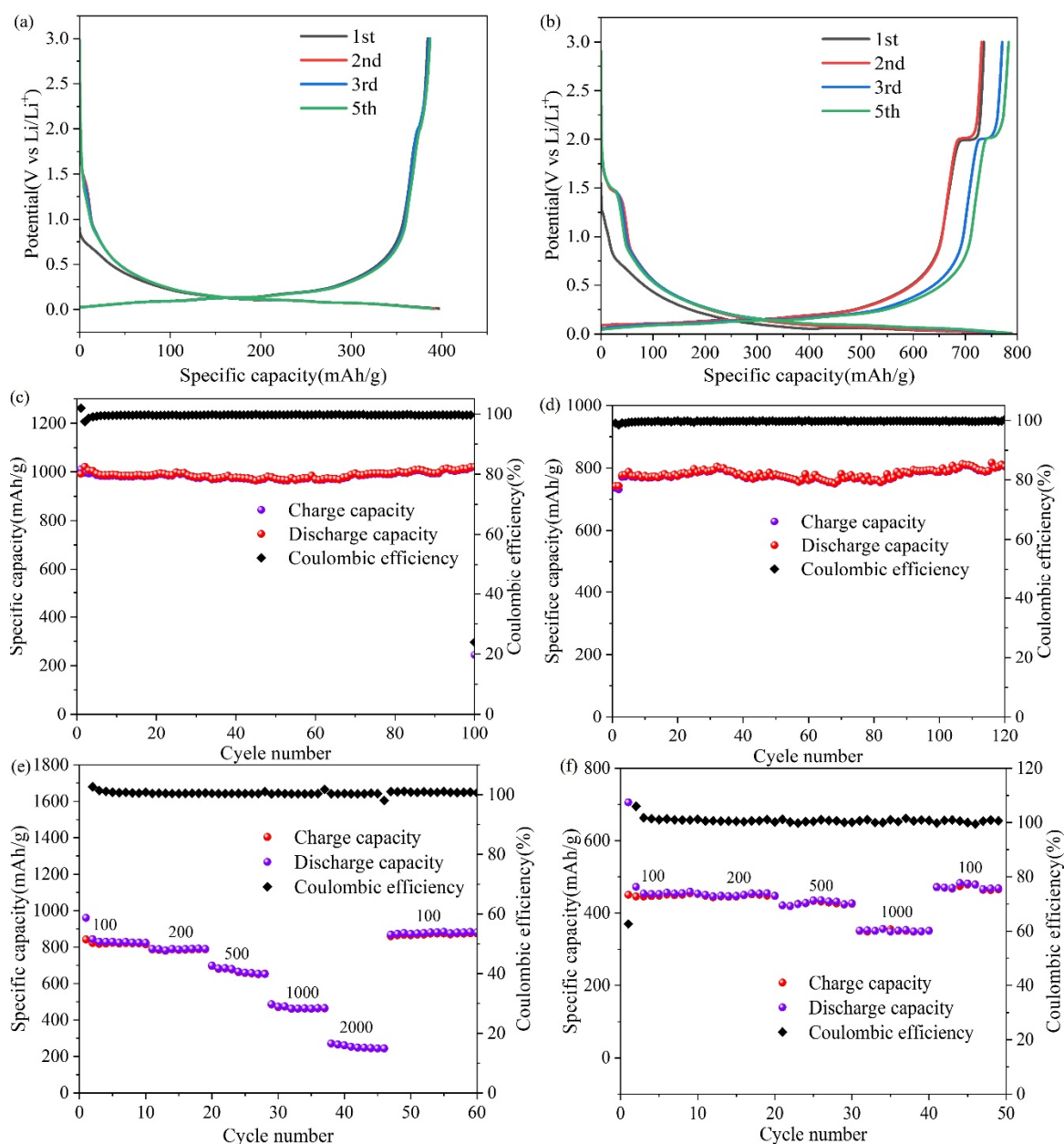


Figure 3. Charge/discharge curves of (a) u-CoSe/CoO/CP and (b) up-CoSe/CoO/CP. Cycling performance of (c) up-CoSe/CoO/CP and (d) u-CoSe/CoO/CP. Rate capability of (e) up-CoSe/CoO/CP and (f) u-CoSe/CoO/CP.

Figure 4a and 4b present the XRD patterns of the as-prepared u-CoO/CoSe and up-CoO/CoSe composite nanoparticles, respectively. Both samples exhibit well-defined diffraction peaks at $2\theta \approx 36.48^\circ$ (111), 42.38° (200), 61.49° (220), 73.66° (311), and 77.52° (222), which match the cubic CoO phase (JCPDS No. 78-0431). Several minor peaks are also observed, confirming the coexistence of the CoSe phase in the composite. Notably, Figure 4b demonstrates that the PEG-modified up-CoO/CoSe retains the characteristic peaks of both CoO and CoSe, indicating successful synthesis while preserving the crystalline structure. The absence of additional impurity phases suggests that PEG incorporation does not compromise the material's phase purity.

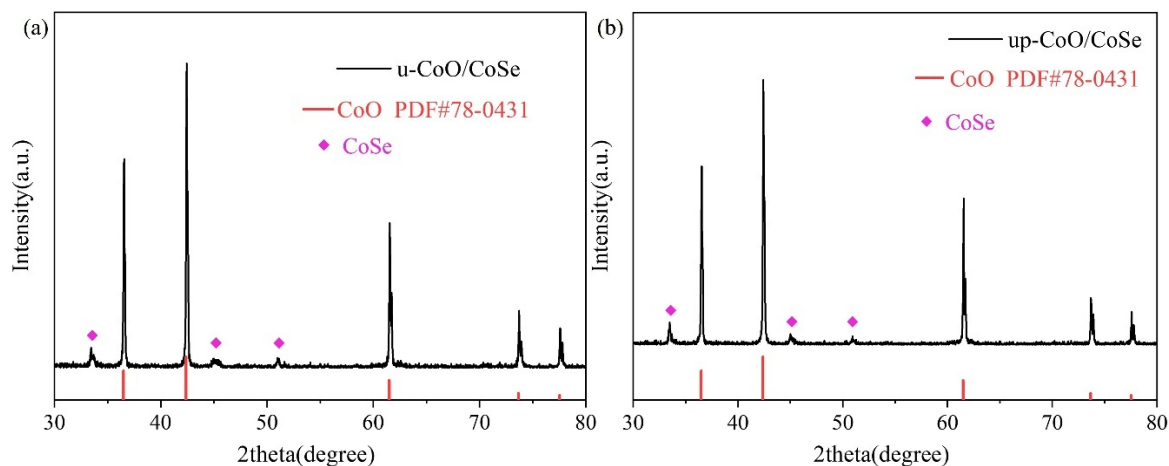


Figure 4. (a) XRD pattern of u-CoSe/CoO and (b) XRD pattern of up-CoSe/CoO.

Figure 5 presents a comparative SEM analysis of u-CoSe/CoO and up-CoSe/CoO nanostructures. In Figure 5a-b, the unmodified u-CoSe/CoO exhibits a rod-like morphology with particle lengths ranging from 200 to 500 nm. The microstructure appears somewhat irregular in size and shape. In contrast, Figure 5c-d reveals that the PEG-modified up-CoSe/CoO maintains a similar rod-like structure but with enhanced uniformity in size and morphology, suggesting that PEG plays a critical role in regulating nanoparticle growth and distribution. This improved structural homogeneity could contribute to better electrochemical performance by providing more consistent active sites and ion diffusion pathways.

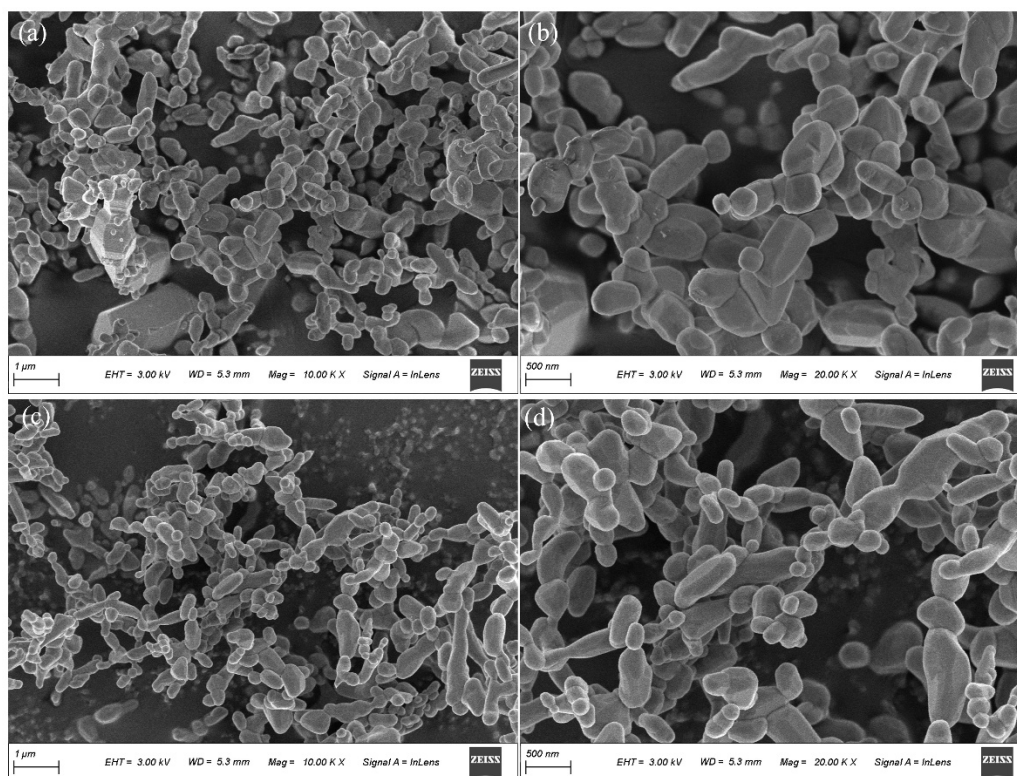


Figure 5. (a)(b) and (c)(d) show the SEM images of (a) u-CoSe/CoO and (b) up-CoSe/CoO at different magnifications, respectively.

Figure 6a presents the galvanostatic charge-discharge profiles of the u-CoSe/CoO electrode. The electrode demonstrates an initial discharge capacity of 480 mAh/g and a charge capacity

of 320 mAh/g, corresponding to a first-cycle Coulombic efficiency (CE) of 66.7%. Notably, compared to u-CoSe/CoO/CP, the pristine u-CoSe/CoO exhibits significantly lower capacity and CE values, highlighting that carbon paper (CP) support effectively: Enhances electrochemical performance, reduces irreversible capacity loss, and improves cycling stability. A similar trend is observed for the PEG-modified samples (Figure 6b). The up-CoSe/CoO electrode delivers an initial discharge capacity of 540 mAh/g and a charge capacity of 370 mAh/g, achieving a higher first-cycle CE of 68.5%. Compared to the PEG-free counterpart, this improvement suggests that PEG incorporation further optimizes the material's electrochemical behavior, likely through enhanced structural uniformity and conductivity.

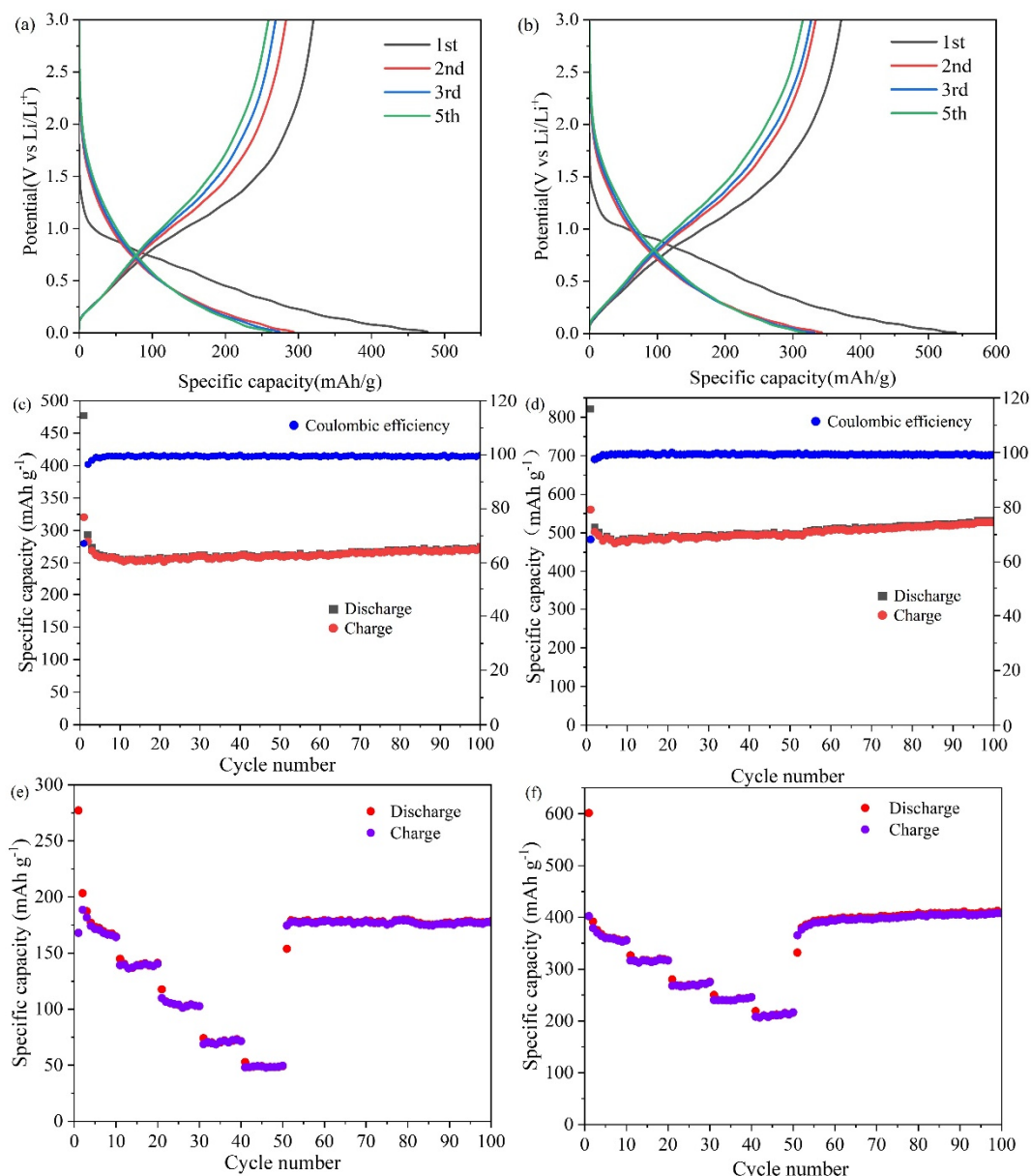


Figure 6. Charge/discharge curves of (a) u-CoSe/CoO and (b) up-CoSe/CoO. Cycling performance of (c) u-CoSe/CoO and (d) up-CoSe/CoO. Rate capability of (e) u-CoSe/CoO and (f) up-CoSe/CoO.

As shown in Figures 6c and 6d, the cycling performance of the u-CoSe/CoO and up-CoSe/CoO electrodes at an current density of 0.1 A/g is presented. As can be seen from Figure 6c, the specific capacity of the u-CoSe/CoO electrode after 100 cycles is approximately 270 mAh/g, and the performance is relatively stable. However, it is lower than that of the u-CoSe/CoO electrode

in Figure 6d (with a specific capacity of about 530 mAh/g after 100 cycles). Compared to u-CoSe/CoO, the PEG-modified sample (up-CoSe/CoO) exhibits a notable increase in capacity, confirming that PEG effectively enhances the material's electrochemical performance. Furthermore, when comparing up-CoSe/CoO/CP, it is evident that the carbon paper-supported sample surpasses up-CoSe/CoO in terms of charge/discharge capacity, Coulombic efficiency, and overall performance, highlighting the beneficial role of carbon paper in optimizing electrode properties. Figure 6e presents the rate capability evaluation of the u-CoO/CoSe electrode. The specific capacities measured at progressively increasing current densities (100, 200, 500, 1000, 2000, and 100 A/mg) demonstrate a stepped-down downward trend (175 → 148 → 110 → 75 → 51 → 175 mAh/g), revealing the material's limited rate capability and poor high-current performance. Figure 6f shows the rate performance of the PEG-modified up-CoO/CoSe electrode. While exhibiting the same capacity decay pattern with increasing current density (370 → 320 → 265 → 240 → 200 → 400 mAh/g), the PEG-modified sample demonstrates 2-3 times higher capacity than its unmodified counterpart across all tested current densities. This contrast highlights the substrate-dependent performance enhancement mechanism of PEG modification, where carbon paper support appears essential for realizing PEG's full potential in improving both capacity and cycling stability.

4. Summary

This study employs a hydrothermal method to grow Co-containing precursor nanoparticles on a carbon paper substrate. Subsequently, the nanoparticles undergo high-temperature selenization in a tube furnace under an argon atmosphere. During this process, the surface of the Co-containing nanoparticles reacts with selenium, forming a CoSe shell while the core remains as CoO, ultimately yielding a CoO/CoSe composite heterostructure. The lithium-ion storage performance of this heterostructure was systematically investigated. For the carbon paper-supported samples (u-CoO/CoSe and up-CoO/CoSe), the introduction of polyethylene glycol (PEG) enhances the CoO/CoSe content and strengthens the synergistic effect within the heterostructure. This modification significantly improves the electrode material's conductivity, mitigates volume expansion issues, and ultimately enhances the battery's lithium storage performance. Furthermore, a comparison between self-supporting electrodes (prepared on carbon paper) and non-self-supporting electrodes reveals that the self-supporting electrodes benefit from the carbon paper's three-dimensional conductive network, which enhances overall electrode conductivity. Additionally, the open-pore structure of the carbon paper effectively buffers the volume expansion of active materials, thereby improving the cycling stability of the battery.

Acknowledgments

This work was financially supported by the Jiangsu Province's "Double Innovation Doctor" project (JSSCBS20221612).

References

- [1] Huizhen Li. Preparation and Investigation of Multiwall Carbon Nanotube Based Electrodes for Efficient Long-life Batteries [D]. Wenzhou University, 2018.
- [2] Armand M, Tarascon J M. Building better batteries. *Nature*, 2008, 451(7179).
- [3] Whittingham M S. The Role of Ternary Phases in Cathode Reactions [J]. *Journal of The Electrochemical Society*, 1976, 123(3):315-320.
- [4] Mizushima K, Jones P C, Goodenough J B, et al. Li_xCoO_2 ($0 < x < 1$): A new cathode material for batteries of high energy Density [J]. *Materials Research Bulletin*, 1980, 15(6): 783-789.

- [5] Poizot, P., Laruelle, S., Grugeon, S. et al. Nano-sized transition-metal oxides as negative-electrode materials for lithium-ion batteries. *Nature* 407, 496–499 (2000).
- [6] Weiyuan H, Qi Z, Mingjian Z, et al. Surface Design with Cation and Anion Dual Gradient Stabilizes High-Voltage LiCoO₂ [J]. *Advanced Energy Materials*, 2022, 12 (20): 2200813.
- [7] Zhang J, Li Z, Lou X W. A freestanding selenium disulfide cathode based on cobalt disulfide-decorated multichannel carbon fibers with enhanced lithium storage performance[J]. *Angewandte Chemie*, 2017, 129(45): 14295-14300.
- [8] Juan Wang, Xianglan Zhang. Research progress on the application of silicon-carbon anode materials in lithium-ion batteries[J]. *Chemical Industry and Engineering*, 2024, 41(06): 75-90.
- [9] Wu X, Li J, Li J, et al. Two-dimensional layered Co₃O₄/CoSe₂ heterostructure modified separator for high-capacity and long-cycle lithium-sulfur Battery [J]. *Journal of Colloid and Interface Science*, 2025, 690: 137366.
- [10] Zhicun Li. Preparation of MOF-Derived Three-Dimensional Carbon Frame and Its Research on Inhibiting Lithium Dendrite Growth[D], Yanshan University, 2024.
- [11] Zhang X, Cai B, Luo Q, et al. Two-step modification strategy enhances carbon fiber/old corrugated container fiber flexible conductive Film [J]. *Diamond and Related Materials*, 2024, 146: 111209.
- [12] Cui L, Qi H, Wang N, et al. N/S co-doped CoSe/C nanocubes as anode materials for Li-ion batteries [J]. *Nanotechnology Reviews*, 2021, 11(1): 244-251.
- [13] Zhou Y, Tian R, Duan H, et al. CoSe/Co nanoparticles wrapped by in situ grown N-doped graphitic carbon nanosheets as anode material for advanced lithium ion batteries[J]. *Journal of Power Sources*, 2018, 399: 223-230.
- [14] Xiaolin Zhang, Bin Cai, Qian Luo, Jiangtao Dang, Xinmei Liu, Xinyue Ma, Two-step modification strategy enhances carbon fiber/old corrugated container fiber flexible conductive film, *Diamond and Related Materials*, Volume 146, 2024, 111209.